

Mid-Holocene El Niño–Southern Oscillation (ENSO) attenuation revealed by individual foraminifera in eastern tropical Pacific sediments

Athanasios Koutavas* Department of Engineering Science and Physics, College of Staten Island, The City University of New York, 2800 Victory Blvd., Staten Island, New York 10314, USA, and Lamont-Doherty Earth Observatory of Columbia University, 61 Rt. 9W, Palisades, New York 10964, USA

Peter B. deMenocal Lamont-Doherty Earth Observatory of Columbia University, 61 Rt. 9W, Palisades, New York 10964, USA

George C. Olive Columbia University, 2960 Broadway, New York, New York 10027, USA

Jean Lynch-Stieglitz School of Earth and Atmospheric Sciences, 311 Ferst Drive, Georgia Institute of Technology, Atlanta, Georgia 30332, USA

ABSTRACT

Holocene reconstructions of the El Niño–Southern Oscillation (ENSO) provide valuable perspective on its recent evolution and can be important for assessing its future. Optimal assessment of past ENSO variability requires observations from its center of action in the eastern equatorial Pacific, but these are limited due to paucity of high-resolution paleoceanographic archives (e.g., corals). Here we use a new approach to quantify past ENSO variance based on the oxygen isotopic composition ($\delta^{18}\text{O}$) of individual foraminifera (*Globigerinoides ruber*) from deep-sea sediments in the ENSO source region. Individual *G. ruber* foraminifera behave as monthly recorders of sea-surface conditions, including ENSO extremes, circumventing the lack of annual resolution in the sediments. Intrapopulation $\delta^{18}\text{O}$ distributions derived with this method from a core near the Galapagos Islands reveal mid-Holocene reductions in variance of 50%, requiring drastic attenuation of the ENSO amplitude. Furthermore, Mg/Ca thermometry indicates that mid-Holocene background conditions were accompanied by a stronger zonal temperature gradient that coincided with a northward-displaced Intertropical Convergence Zone (ITCZ). The results suggest that the position of the ITCZ is an important factor in the low-frequency modulation of ENSO and could influence its future evolution.

Keywords: Holocene ENSO, ITCZ, tropical Pacific, individual *G. ruber*, oxygen isotopes.

INTRODUCTION

Sensible and latent heating of the atmosphere over marine regions of atmospheric convection are important sources of energy for the global circulation, and for this reason, tropical sea-surface temperatures (SSTs) constitute major determinants of worldwide climatic patterns (Battisti et al., 1999). El Niño–Southern Oscillation (ENSO) produces large year-to-year changes in tropical Pacific SSTs causing widespread climate anomalies (Halpert and Ropelewski, 1992). Despite recent progress in understanding the interannual aspects of ENSO, there is ongoing debate concerning its dynamics over longer time scales. It is thought that the coupled ocean-atmosphere system may exhibit low-frequency modes of variability that mimic ENSO but operate on time scales from millennia to millions of years (e.g., Clement et al., 1999; Philander and Fedorov, 2003). The basic characteristics of such long-period adjustments, their relation to interannual ENSO, and links with global climate remain elusive. Here, we examine tropical Pacific climate progression over the course of the Holocene, a period of growing interest due to evidence for large changes in ENSO behavior and cen-

tral relevance for future ENSO evolution (Cane, 2005). We present evidence for (1) inverse Holocene SST trends in the eastern and western Pacific from Mg/Ca thermometry, and (2) strongly attenuated mid-Holocene ENSO from $\delta^{18}\text{O}$ distributions of individual foraminifera.

MATERIALS AND METHODS

Mg/Ca ratios were measured on tests of the surface-dwelling species *Globigerinoides ruber* picked from the 250–355 μm size fraction in cores V21–30 (1°13'S, 89°41'W, 617 m) and V19–28 (2°22'S, 84°39'W, 2720 m) (Fig. 1). Approximately 100 tests per sample in V21–30 (50 in V19–28) were aggregated, lightly crushed, mixed, and split in 2–3 aliquots for replicate Mg/Ca analyses and stable isotope work. Splits for Mg/Ca underwent clay removal and oxidative and reductive cleaning following procedures described previously (Koutavas et al., 2002). Analyses were made with a Jobin Yvon Panorama 2000 inductively coupled plasma–optical emission spectrometer (ICP-OES). Sample reproducibility based on replicate analyses was ± 0.065 mmol/mol, equivalent to $\pm 2\%$ or ± 0.23 °C. Temperature was calculated with the equation $T(^{\circ}\text{C}) = \ln(\text{Mg}/\text{Ca}[\text{mmol}/\text{mol}]/0.38)/0.09$ (DeKens et al., 2002).

For $\delta^{18}\text{O}$, one split of the crushed sample (1/3 of ~ 100 shells) was analyzed with a Micromass Optima stable isotope mass spectrometer equipped with Multiprep. The 1σ analytical error was $\pm 0.06\text{‰}$ based on repeat analyses of NBS-19 and a working standard. The $\delta^{18}\text{O}$ of individual *G. ruber* was measured on tests from the 300–355 μm size fraction with 1σ error of $\pm 0.1\text{‰}$ (somewhat high because these small analyses were close to the operational limit of the instrument). Age control was based on three ^{14}C ages in V21–30 and two ^{14}C ages in V19–28 (Koutavas and Lynch-Stieglitz, 2003).

HOLOCENE TRENDS IN TROPICAL PACIFIC SST FROM Mg/Ca THERMOMETRY

Sites V21–30 and V19–28 lie in the region of minimum SSTs associated with divergent upwelling in the equatorial cold tongue (Fig.

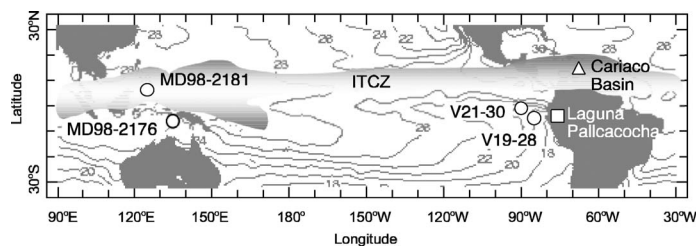


Figure 1. Map of tropical Pacific Ocean showing locations of cores used in this study. Background sea-surface temperatures (SSTs) correspond to La Niña conditions during August 1999. Approximate position of Intertropical Convergence Zone (ITCZ) was drawn using satellite cloud composites from 2 August 1999, available at <http://www.ssec.wisc.edu/data>.

*E-mail: koutavas@mail.csi.cuny.edu.

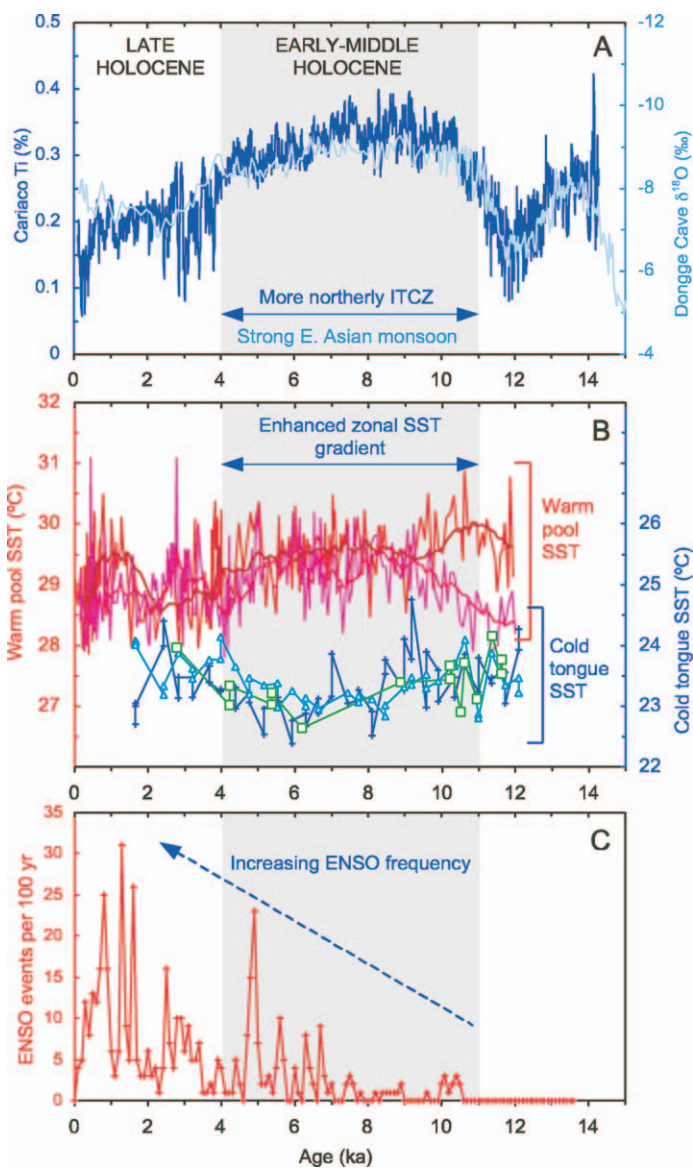


Figure 2. Holocene Mg/Ca sea-surface temperature (SST) reconstructions from equatorial Pacific compared with records of Intertropical Convergence Zone (ITCZ), East Asian monsoon, and El Niño–Southern Oscillation (ENSO). A: Titanium (%) in Ocean Drilling Project (ODP) Site 1002C from the Cariaco Basin (dark blue) (Haug et al., 2001); $\delta^{18}\text{O}$ of the D4 stalagmite from Dongge Cave, China (light blue) (Yuan et al., 2004). B: Mg/Ca SSTs from the western Pacific warm pool and eastern Pacific cold tongue: *G. ruber* SST from MD98–2181 (red) and MD98–2176 (pink) (Stott et al., 2004); *G. ruber* SST from V21–30 (blue crosses) and V19–28 (green open squares; adjusted by +1.7 °C) (this study); *G. sacculifer* Mg/Ca SST from V21–30 (blue open triangles; adjusted by +1.2 °C) (Koutavas et al., 2002). Bold lines through warm pool SST records are smoothed versions of raw data. C: Holocene ENSO frequency from Laguna Pallcacocha (Ecuador) sediment color intensity (Moy et al., 2002).

1) and have average sedimentation rates of 13.4 and 5.6 cm/k.y., respectively, which are among the highest in the region (Koutavas and Lynch-Stieglitz, 2003). Site V21–30 is especially well suited for this work because its shallow depth minimizes overprinting effects due to calcite dissolution, which confound the Mg/Ca and $\delta^{18}\text{O}$ proxies (Rosenthal and Lohmann, 2002). Although deeper and lower in resolution, the record of nearby V19–28 is strongly correlated with that of V21–30, indicating regional coherence. *G. ruber* Mg/Ca SSTs are shown in Figure 2B, together with the previously published *G. sacculifer* record from V21–30 (Koutavas et al., 2002). Presently, these three data series

comprise the best available index of Holocene SST progression in the equatorial Pacific cold tongue.

We compared our SST records from the eastern Pacific with those obtained from two high-resolution sites in the western Pacific warm pool, MD98–2181 and MD98–2176 (Fig. 1), which were also based on the Mg/Ca ratio of *G. ruber* and employed the same calibration equation (Stott et al., 2004). The comparison (Fig. 2B) reveals fundamental east-west differences that amount to distinct and nearly opposite Holocene climate trends. The three sequences from the cold tongue uniformly reflect a broad interval of cooler conditions between 9 and 5 ka, a time when western Pacific SSTs indicate peak Holocene warmth. A notable feature of the inverse east-west temperature trends occurs around 4–5 ka, when the eastern Pacific sites undergo a warming of ~ 0.5 °C, while both sites from the west reflect a cooling of comparable magnitude. This time horizon (4.5 ± 0.5 ka) marks the end of the anomalous mid-Holocene interval and the transition to a late Holocene climate regime more typical of present-day conditions. The combined mid-Holocene anomalies amount to an average increase of the zonal SST gradient by ~ 1 °C, a 20% increase over the modern value of 5 °C. Ca. 6 ka, the zonal gradient was ~ 1.5 °C, or 30% higher than modern. These anomalies resemble the modern spatial pattern of the cold phase of ENSO (La Niña) and imply a stronger Walker circulation and enhanced Bjerknes feedback. Considering that the proxy data by construction represent multidecadal averages, these changes appear sufficiently large to have been globally important.

The Role of the Intertropical Convergence Zone

The origin of the anomalous mid-Holocene state may have been either oceanic (for example, through changes in the depth of the equatorial thermocline), or atmospheric (involving changes in the equatorial wind field). Here, we draw attention to a potential atmospheric mechanism involving changes in the location of the Intertropical Convergence Zone (ITCZ) (Fig. 1). It draws on current understanding of seasonal and interannual upwelling and SST variations in the cold tongue, which are coupled to the position of the marine ITCZ (Mitchell and Wallace, 1992; Deser and Wallace, 1990; Raymond et al., 2004). Peak divergence and surface cooling occur in August–September during the ITCZ's northern extreme ($\sim 10^\circ\text{N}$), which brings the equator under the influence of strong southeast trades (Mitchell and Wallace, 1992). Cold ENSO episodes are similarly accompanied by anomalous northerly ITCZ shifts, and the opposite is true of warm episodes (Deser and Wallace, 1990). By analogy, the mid-Holocene changes could have resulted from a northward-displaced marine ITCZ favoring more permanent southeast trades and promoting cool upwelling.

Direct Holocene ITCZ constraints from the Pacific are unavailable to test this hypothesis. However, the hydrologic record of the Cariaco Basin in the western tropical Atlantic (Haug et al., 2001) is particularly relevant because of its proximity to the eastern Pacific (Fig. 1). Elevated concentrations of continentally derived titanium in Cariaco sediments (Fig. 2A) are thought to reflect a northward-displaced Atlantic ITCZ in the early-middle Holocene. The timing of this displacement coincides with the inverse SST variations in the eastern and western Pacific (Fig. 2B), which supports a link between the SST trends and the position of the ITCZ, and may further help explain the salinity enrichment observed in the western Pacific (Stott et al., 2004). If correct, this mechanism implies that broad-scale Holocene ITCZ shifts previously recognized in the Atlantic (Haug et al., 2001) and Indian Oceans (Fleitmann et al., 2003) also occurred in the Pacific, most likely as part of a global atmospheric adjustment to orbital forcing. Notably, this adjustment included an intensified East Asian summer monsoon (Yuan et al., 2004) (Fig. 2A), which is likely to have been reinforced by the anomalous tropical Pacific SSTs.

DEDUCING ENSO FROM INDIVIDUAL *G. RUBER*

Modeling has indicated drastic reduction of mid-Holocene ENSO activity (Clement et al., 2000), supported by evidence from Papua New Guinea corals (Tudhope et al., 2001) and lake sediments from Ecuador (Moy et al., 2002) (Fig. 2C). While important, these observations assumed stationary ENSO teleconnections, complicating efforts to quantify the implied ENSO changes.

Given the dearth of Holocene ENSO archives from the equatorial cold tongue, we employed a novel approach to assess ENSO variability from open ocean sediments. It utilizes the $\delta^{18}\text{O}$ of individual tests of *G. ruber* isolated from narrow sediment intervals in core V21–30 near the Galapagos Islands (Fig. 1). Individual *G. ruber* have average life spans of 2–4 wk (Spero, 1998), acting as near-monthly recorders of sea-surface conditions. For this reason, the isotopic range and variance within a fossil population is diagnostic of the hydrographic variability at the time of deposition. The $\delta^{18}\text{O}$ of *G. ruber* is primarily controlled by SST (-0.21‰) (Bemis et al., 1998) and secondarily by sea-surface salinity (SSS) (0.27‰) (Fairbanks et al., 1982). In the Galapagos region, as in most of the tropics, SST and SSS are inversely related because positive SST excursions drive increased precipitation that lowers the salinity. As a result, the $\delta^{18}\text{O}$ of calcite formed during El Niño episodes (positive SST and negative SSS anomalies) is strongly depleted, and, conversely, during La Niña it is enriched. Thus, the overall distribution of $\delta^{18}\text{O}$ in a sediment sample provides a measure of the ENSO frequency and amplitude within the deposition window. This method relies on the assumption that *G. ruber* can tolerate the full range of SST and SSS over the large annual cycle and during peak ENSO events. Results from the core-top samples of V21–30 (presented in the following paragraphs) support this assumption.

We analyzed individual *G. ruber* foraminifera from two late Holocene and two mid-Holocene intervals in core V21–30 and compared their distributions. Each 1-cm-wide sample nominally represents an ~ 75 yr window, although the true interval is likely longer due to bioturbation. Individual analyses from the core-top sample ($n = 52$) dated by ^{14}C to 1.7 ka revealed a remarkably wide overall $\delta^{18}\text{O}$ range of 2.4‰ (Fig. 3). The seasonal amplitudes of SST (5 °C) and SSS (1.3 psu) at this site today account for 1.4‰ in $\delta^{18}\text{O}$, leaving 1‰ to be explained by ENSO variability, which is consistent with expectations from climatologic SST and SSS variations over a full ENSO cycle (Fig. 3). The large $\delta^{18}\text{O}$ range in the data is itself noteworthy and supports a broad temperature and salinity tolerance for *G. ruber* foraminifera and their ability to survive and record extreme ENSO events. We suspect that this is a consequence of the unique environment of the cold tongue, which allows *G. ruber* to exploit opposite oceanographic extremes due to (1) favorable temperature and salinity during warm events, or (2) abundant food resources during cold events. A second sample from a depth of 10 cm (2.4 ka) gave a similar $\delta^{18}\text{O}$ range of 2.2‰ ($n = 41$). In each of the two late Holocene samples, the individual $\delta^{18}\text{O}$ data are distributed normally with mean and 1σ values of -1.72‰ (± 0.51) and -1.76‰ (± 0.44).

We turned next to the mid-Holocene and analyzed individuals from 55 and 60 cm depth, dated to 5.9 and 6.3 ka. In both samples, the $\delta^{18}\text{O}$ distributions were distinctly narrower (Fig. 3). The 5.9 ka sample yielded a total range of 1.3‰ ($n = 49$), and the 6.3 ka sample yielded 1.7‰ ($n = 47$). The mean and 1σ values were -1.67‰ (± 0.31) and -1.77‰ (± 0.36), respectively.

Statistical comparison of the pooled $\delta^{18}\text{O}$ data from the late ($n = 93$) and mid-Holocene ($n = 96$) reveals a decrease in total variance of 50%, significant at 99% confidence (Fig. 3). Although the $\delta^{18}\text{O}$ variance incorporates both seasonal and interannual components, this decrease appears too large to be explained solely by a dampened seasonal cycle; our calculations show that this would require $>60\%$ amplitude attenuation of seasonal SST and SSS variations. Given the modern

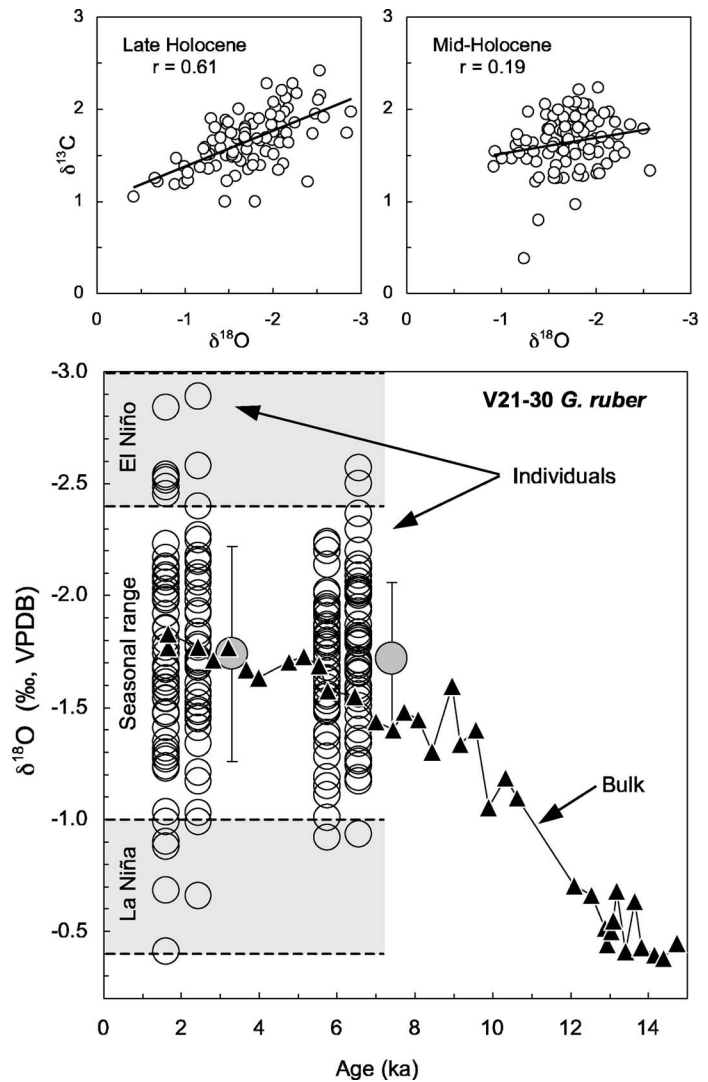


Figure 3. $\delta^{18}\text{O}$ of individual *G. ruber* (open circles) from core V21–30. Black triangles are downcore $\delta^{18}\text{O}$ data from same site measured on bulk *G. ruber* samples. Filled circles with error bars indicate mean and standard deviation of pooled individuals from late ($n = 93$) and mid-Holocene ($n = 96$). Standard deviation of mid-Holocene pool ($\sigma = 0.34$) is 30% less than late Holocene ($\sigma = 0.48$), and total variance (σ^2) is 50% less, significant at 99% confidence. Gray shading marks predicted $\delta^{18}\text{O}$ ranges due to seasonal and El Niño–Southern Oscillation (ENSO) variations, calculated with low-light equation of Bemis et al. (1998) and seawater $\delta^{18}\text{O}$ –salinity relationship of Fairbanks et al. (1982) using World Ocean Atlas 01 and Integrated Global Ocean Services System (IGOSS) sea-surface temperature (SST) and sea-surface salinity (SSS) data available from <http://iridl.ldeo.columbia.edu>. $\delta^{18}\text{O}$ – $\delta^{13}\text{C}$ scatter plots of pooled individuals are shown at top. VPDB—Vienna Pee Dee belemnite.

dependence of ENSO on seasonality (Chang et al., 1995), we suggest that the most plausible interpretation calls for equivalent contributions by both ENSO and the seasonal cycle to the observed reduction in total variance.

Comparison of $\delta^{18}\text{O}$ with carbon isotopic ratios ($\delta^{13}\text{C}$) of the same samples (Fig. 3) further supports an upwelling mechanism for the mid-Holocene decrease in variance. Cool upwelling waters are rich in nutrients and depleted in $\delta^{13}\text{C}$, which results in negatively correlated $\delta^{18}\text{O}$ and $\delta^{13}\text{C}$ values at times of large upwelling variability (i.e., strong ENSO). In the late Holocene, $\delta^{18}\text{O}$ and $\delta^{13}\text{C}$ are indeed strongly anticorrelated ($r = 0.61$), whereas in the mid-Holocene there is lack of significant correlation ($r = 0.19$). This implies that mid-Holocene variations were only weakly tied to upwelling and therefore are less likely

to be ENSO related. As a whole, the isotopic data confirm a significant dampening of ENSO during the mid-Holocene directly from the marine environment of the eastern Pacific.

IMPLICATIONS FOR FUTURE ENSO

Our results suggest that the anomalous mid-Holocene tropical Pacific state involved a northward displacement of the ITCZ favorable to equatorial divergence. In this view, the mid-Holocene ENSO attenuation was the result of more sustained southeast trades and a steadier equatorial upwelling regime. Southward retreat of the ITCZ in the late Holocene would have increased instability and amplified the potential for westerly wind anomalies needed to initiate El Niño events. While the mid-Holocene ITCZ and ENSO anomalies most likely had an orbital source (Haug et al., 2001; Clement et al., 2000), recent modeling suggests that the marine ITCZ is also sensitive to high-latitude processes such as ice cover (Chiang and Bitz, 2005) and thermohaline circulation (Zhang and Delworth, 2005), both of which are deemed vulnerable to future climate change (Overpeck et al., 2005). In this regard, the future response of the ITCZ to changing climate and its potential to interact with ENSO merit careful consideration. Presently, climate model skill in simulating the equatorial Pacific cold tongue–ITCZ complex is weak (Raymond et al., 2004), and this imposes limitations in ability to evaluate long-term ENSO–ITCZ interactions. The mid-Holocene reconstructions presented here provide a useful target for model validation experiments toward improved understanding of tropical Pacific climate variability, past and future.

ACKNOWLEDGMENTS

We thank Lowell Stott and an anonymous reviewer for thoughtful comments; H. Griffith and G. Kim for technical assistance; and W.B.F. Ryan for a summer internship to G.C. Olive. Funding was provided by the National Science Foundation (NSF) grant OCE04–02478, by a grants/cooperative agreement from the National Oceanic and Atmospheric Administration (NOAA), and by the Lamont-Doherty Earth Observatory (LDEO) Climate Center. A. Koutavas was supported by a NOAA postdoctoral fellowship in Climate and Global Change, administered by the University Corporation for Atmospheric Research. Sample material was provided by the LDEO deep-sea sample repository. Support for the collection and curating facilities of the core repository is provided by NSF through grant OCE03–50504 and the Office of Naval Research through grant N00014-03-1-0722.

REFERENCES CITED

- Battisti, D.S., Sarachik, E.S., and Hirst, A.C., 1999, A consistent model of the large-scale steady surface atmospheric circulation in the tropics: *Journal of Climate*, v. 12, p. 2956–2964, doi: 10.1175/1520-0442(1999)012<2956:ACMFTL>2.0.CO;2.
- Bemis, B.E., Spero, H.J., Bijma, J., and Lea, D.W., 1998, Reevaluation of the oxygen isotopic composition of planktonic foraminifera: Experimental results and revised paleotemperature equations: *Paleoceanography*, v. 13, p. 150–160, doi: 10.1029/98PA00070.
- Cane, M.A., 2005, The evolution of El Niño, past and future: *Earth and Planetary Science Letters*, v. 230, p. 227–240, doi: 10.1016/j.epsl.2004.12.003.
- Chang, P., Ji, L., Wang, B., and Li, T., 1995, Interactions between the seasonal cycle and El Niño–Southern Oscillation in an intermediate coupled ocean–atmosphere model: *Journal of Atmospheric Sciences*, v. 52, p. 2353–2372, doi: 10.1175/1520-0469(1995)052<2353:IBTSCA>2.0.CO;2.
- Chiang, J.C.H., and Bitz, C.M., 2005, Influence of high latitude ice cover on the marine Intertropical Convergence Zone: *Climate Dynamics*, v. 25, p. 477–496, doi: 10.1007/s00382-005-0040-5.
- Clement, A.C., Seager, R., and Cane, M.A., 1999, Orbital controls on the El Niño/Southern Oscillation and the tropical climate: *Paleoceanography*, v. 14, p. 441–456, doi: 10.1029/1999PA900013.
- Clement, A.C., Seager, R., and Cane, M.A., 2000, Suppression of El Niño during the mid-Holocene by changes in the Earth's orbit: *Paleoceanography*, v. 15, p. 731–737, doi: 10.1029/1999PA000466.
- Dekens, P., Lea, D.W., Pak, D.K., and Spero, H.J., 2002, Core top calibration of Mg/Ca in tropical foraminifera: Refining paleotemperature estimation: *Geochemistry, Geophysics, Geosystems*, v. 3, doi: 10.1029/2001GC002000.
- Deser, C., and Wallace, J.M., 1990, Large-scale atmospheric circulation features of warm and cold episodes in the tropical Pacific: *Journal of Climate*, v. 3, p. 1254–1281, doi: 10.1175/1520-0442(1990)003<1254:LSACFO>2.0.CO;2.
- Fairbanks, R.G., Sverdrlove, M., Free, R., Wiebe, P.H., and Bé, A.W.H., 1982, Vertical distribution and isotopic fractionation of living planktonic foraminifera from the Panama Basin: *Nature*, v. 298, p. 841–844, doi: 10.1038/298841a0.
- Fleitmann, D., Burns, S.J., Mudelsee, M., Neff, U., Kramers, J., Mangini, A., and Matter, A., 2003, Holocene forcing of the Indian monsoon recorded in a stalagmite from Southern Oman: *Science*, v. 300, p. 1737–1739, doi: 10.1126/science.1083130.
- Halpert, M.S., and Ropelewski, C.F., 1992, Surface temperature patterns associated with the Southern Oscillation: *Journal of Climate*, v. 5, p. 577–593, doi: 10.1175/1520-0442(1992)005<0577:STPAWT>2.0.CO;2.
- Haug, G.H., Hughen, K.A., Sigman, D.M., Peterson, L.C., and Röhl, U., 2001, Southward migration of the Intertropical Convergence Zone through the Holocene: *Science*, v. 293, p. 1304–1308, doi: 10.1126/science.1059725.
- Koutavas, A., and Lynch-Stieglitz, J., 2003, Glacial-interglacial dynamics of the eastern equatorial Pacific cold tongue–Intertropical Convergence Zone system reconstructed from oxygen isotope records: *Paleoceanography*, v. 18, doi: 10.1029/2003PA000894.
- Koutavas, A., Lynch-Stieglitz, J., Marchitto, T.M., and Sachs, J.P., 2002, El Niño-like pattern in ice age tropical Pacific sea surface temperature: *Science*, v. 297, p. 226–230, doi: 10.1126/science.1072376.
- Mitchell, T.P., and Wallace, J.M., 1992, The annual cycle of equatorial convection and sea surface temperature: *Journal of Climate*, v. 5, p. 1140–1156, doi: 10.1175/1520-0442(1992)005<1140:TACIEC>2.0.CO;2.
- Moy, C.M., Seltzer, G.O., Rodbell, D.T., and Anderson, D.M., 2002, Variability of El Niño/Southern Oscillation activity at millennial time scales during the Holocene epoch: *Nature*, v. 420, p. 162–165, doi: 10.1038/nature01194.
- Overpeck, J.T., and 20 others, 2005, Arctic system on trajectory to new, seasonally ice-free state: *Eos (Transactions, American Geophysical Union)*, v. 86, p. 309–313.
- Philander, S.G., and Fedorov, A.V., 2003, Role of tropics in changing the response of Milankovitch forcing some three million years ago: *Paleoceanography*, v. 18, doi: 10.1029/2002PA000837.
- Raymond, D.J., Esbensen, S.K., Paulson, C., Gregg, M., Bretherton, C.S., Petersen, W.A., Cifelli, R., Shay, L.K., Ohlmann, C., and Zuidema, P., 2004, EPIC2001 and the coupled ocean–atmosphere system of the tropical east Pacific: *Bulletin of the American Meteorological Society*, v. 85, p. 1341–1354, doi: 10.1175/BAMS-85-9-1341.
- Rosenthal, Y., and Lohmann, G.P., 2002, Accurate estimation of sea surface temperatures using dissolution-corrected calibrations for Mg/Ca paleothermometry: *Paleoceanography*, v. 17, doi: 10.1029/2001PA000749.
- Spero, H.J., 1998, Life history and stable isotope geochemistry of planktonic foraminifera, in Norris, R.D., and Corfield, R.M., eds., *Isotope paleobiology and paleoecology*: Pittsburgh, Pennsylvania, Paleontological Society Papers, v. 4, p. 7–36.
- Stott, L., Cannariato, K., Thunell, R., Haug, G., Koutavas, A., and Lund, S., 2004, Decline of surface temperature and salinity in the western tropical Pacific Ocean in the Holocene epoch: *Nature*, v. 431, p. 56–59, doi: 10.1038/nature02903.
- Tudhope, A.W., Chilcott, C.P., McCulloch, M.T., Cook, E.R., Chappell, J., El-Lam, R.M., Lea, D.W., Lough, J.M., and Shimmield, G.B., 2001, Variability in the El Niño–Southern Oscillation through a glacial-interglacial cycle: *Science*, v. 291, p. 1511–1517, doi: 10.1126/science.1057969.
- Yuan, D., Cheng, H., Edwards, R.L., Dykoski, C.A., Kelly, M.J., Zhang, M., Qing, J., Lin, Y., Wang, Y., Wu, J., Dorale, J.A., An, Z., and Cai, Y., 2004, Timing, duration, and transitions of the last interglacial Asian monsoon: *Science*, v. 304, p. 575–578, doi: 10.1126/science.1091220.
- Zhang, R., and Delworth, T.L., 2005, Simulated tropical response to a substantial weakening of the Atlantic thermohaline circulation: *Journal of Climate*, v. 18, p. 1853–1860, doi: 10.1175/JCLI3460.1.

Manuscript received 25 March 2006

Revised manuscript received 16 June 2006

Manuscript accepted 20 June 2006

Printed in USA